THE ANATOLIAN JOURNAL OF CARDIOLOGY

Official journal of the TURKISH SOCIETY OF CARDIOLOGY

Vericiguat Alleviates Atrial Electrical and Structural Remodeling in Rats with Atrial Fibrillation

ABSTRACT

Background: The initiation and maintenance of atrial fibrillation (AF) are predominantly driven by progressive atrial structural remodeling, characterized by fibrosis and electrical conduction abnormalities. While vericiguat has shown efficacy in attenuating cardiac remodeling in heart failure (HF), its impact on AF remains insufficiently characterized.

Methods: This study investigated the cardioprotective effects of vericiguat in a Sprague-Dawley rat model of AF. Twenty-four male SD rats (250-300 g, 8-10 weeks old) were randomly assigned to control, AF, and vericiguat-treated groups. Echocardiography and histological assessments were performed, along with quantification of NT-proBNP, Collagen I, CaMKII, Cx43, ATG7, P62, and LC3II/I in the left atrium.

Results: Compared to controls, AF rats exhibited atrial enlargement, elevated myocardial fibrosis, and significant alterations in molecular markers. Vericiguat treatment effectively reversed these pathological changes. Specifically, NT-proBNP, Collagen I, CaMKII, ATG7, and LC3II/I were upregulated, while Cx43 and P62 were downregulated in the AF group—changes that were mitigated by vericiguat.

Conclusion: Collectively, these findings suggest that vericiguat attenuates atrial remodeling and AF progression by modulating autophagy and suppressing fibrosis.

Keywords: Atrial fibrillation, autophagy, electrical remodeling, structural remodeling, vericiguat

INTRODUCTION

Atrial fibrillation (AF) is the most prevalent sustained cardiac arrhythmia and is strongly associated with increased risks of ischemic stroke, systemic thromboembolism, and heart failure (HF) progression, thereby contributing substantially to the global cardiovascular disease burden. The 2024 European Society of Cardiology (ESC) guidelines project a twofold rise in AF prevalence over the coming decades, driven primarily by population aging and advances in diagnostic technologies. Atrial fibrillation (AF) has become a notable public health concern.[1,2] Current AF management strategies focus largely on pharmacological rate control and complication prevention, with catheter ablation as the primary interventional option.[3] However, the high recurrence rate and therapeutic resistance of AF post-ablation impose significant economic and societal burdens, underscoring its status as a global health challenge.[4,5] Consequently, elucidating the pathophysiological mechanisms underlying AF and translating these insights into targeted therapies remains a critical unmet need in cardiovascular medicine.

Atrial fibrillation (AF) pathogenesis is fundamentally driven by tightly coupled electrical and structural remodeling processes within the atrial myocardium,[6] although the precise molecular underpinnings remain incompletely defined. Electrical remodeling is characterized by disrupted calcium handling, shortened action potential duration (APD), and impaired conduction. Structural remodeling, in contrast, involves interstitial fibrosis and atrial enlargement—particularly left atrial dilation, which is now recognized as an independent risk factor for AF initiation and maintenance.[7,8] Emerging evidence implicates dysregulated autophagy

ORIGINAL INVESTIGATION

Xia Zhang[1]
Yubing Wang[1]
Liangchen Shen[1]
Zhuang Shuai[1]
Wei Liu[1]
Qian Wen[1]
Hu Tang[1]
Yumei Chen[1]
You Yang[2]
Hanmei Li[2]

[1]*Department of Cardiovascular Medicine, Affiliated Hospital of North Sichuan Medical College, Nanchong, China*
[2]*Department of Ultrasound Medicine, Affiliated Hospital of North Sichuan Medical College, Nanchong, China*

Corresponding author:
Yubing Wang
✉ 495720873@qq.com

Received: September 24, 2025
Accepted: January 28, 2026
Available Online Date: March 13, 2026

Cite this article as: Zhang X, Wang Y, Shen L, et al. Vericiguat alleviates atrial electrical and structural remodeling in rats with atrial fibrillation. *Anatol J Cardiol.* 2026;XX(X):X-X.

DOI: 10.14744/AnatolJCardiol.2026.5822

as a contributing factor in both electrical and structural remodeling,[9,10] suggesting that modulation of autophagy may offer a novel therapeutic avenue for AF.

Vericiguat, a soluble guanylate cyclase stimulator approved for HF treatment, mitigates oxidative stress in cardiomyocytes, exerts anti-fibrotic effects, and improves ventricular remodeling.[11] Large-scale clinical trials have demonstrated that vericiguat provides clinical benefit in HF patients with comorbid AF,[12] although the underlying mechanisms remain unclear. Preclinical and clinical data indicate that vericiguat reduces both electrical and structural remodeling in the ventricles.[13-16] Building upon this foundation, the present study investigated whether vericiguat attenuates atrial remodeling in AF-induced Sprague–Dawley rats and explored its potential regulatory role in atrial autophagy.

METHODS

Establishment of Atrial Fibrillation Rat Model

All SD rats were housed under standardized conditions: temperature 23.0 ± 0.5°C, humidity 50%-60%, and a 12-hour light/dark cycle. Atrial fibrillation (AF) was induced using a modified protocol based on references.[17,18] Rats received daily tail vein injections of a mixed solution containing acetylcholine (ACh, 66 μg/mL; A111014, Aladdin) and $CaCl_2$ (10 mg/mL; 499609, Sigma-Aldrich) for 14 consecutive days. Control rats received an equivalent volume of saline (1 mL/kg) via the same route. Fourteen days after the establishment of the AF model, animals were randomly divided into three groups (n = 8 each): Control, saline via oral gavage; AF, AF induction plus saline gavage; and AF + Vericiguat, AF induction followed by vericiguat 0.5 mg/kg/day (Bayer, USA) via oral gavage for four weeks.[19-21]

Electrocardiographic Analysis and Recording

Anesthesia was induced via intraperitoneal injection of sodium pentobarbital (40 mg/kg). Electrocardiographic monitoring (12-lead ECG, ECG-2303B; Guangzhou Sanrui Electronics Co., Ltd., China) was performed by attaching limb leads to the extremities. Continuous intravenous infusion of ACh-$CaCl_2$ was administered for 14 days, with daily assessments of AF duration. Atrial fibrillation (AF) was confirmed by continuous ECG monitoring, characterized by irregular RR intervals, absence of P-waves, and presence of fibrillatory wave (f-wave) patterns.[18]

Echocardiography Analysis

Cardiac structure and function were evaluated after four weeks using transthoracic echocardiography (LOGIQ E11, GE, USA). Parameters measured included left atrial anteroposterior diameter (LAD), left ventricular ejection fraction (LVEF), and fractional shortening (FS).

Biochemical Assessment

Blood samples were collected, centrifuged, and the serum was stored at −80°C. NT-proBNP concentrations were measured using a commercial enzyme-linked immunosorbent assay kit (ZC-36153, Zhuocai Biotechnology Co., Ltd., Shanghai, China). Absorbance was recorded using a microplate reader (SpectraMax iD3, Molecular Devices Co., Ltd., Shanghai, China).

Histological Staining (Hematoxylin and Eosin and Masson's Trichrome)

Left atrial tissues were fixed, embedded, and sectioned for histological analysis. Sections were stained with hematoxylin and eosin (H&E) or Masson's trichrome, followed by sequential dehydration in graded ethanol, xylene clearing, and mounting with resinous medium. Whole-slide scanning was performed using a digital scanner (Pannoramic 250, 3DHISTECH, Hungary). Representative fields at 400× magnification were imaged to assess tissue morphology and fibrosis. Fibrotic area was quantified using ImageJ software (version 1.8.0, NIH), and calculated as:

$$\text{Fibrosis area fraction (\%)} = (\text{collagen fiber area} / \text{total area}) \times 100.$$

Immunohistochemistry

For immunohistochemical analysis, sections were deparaffinized, rehydrated, and cooled. Antigen retrieval was performed with 3% H_2O_2 for 25 min at room temperature in the dark, followed by three PBS washes (5 minutes each). Sections were incubated overnight at 4°C with primary antibodies in blocking buffer: collagen I (1:200, AF7001, Affinity), ATG7 (1:1000, ET1610-53, HuaAn), and LC3B (1 μg/mL, ab192890, Abcam). After phosphate-buffered saline (PBS) rinsing, horseradish peroxidase (HRP)-conjugated secondary antibodies were applied at 37°C for 30 minutes. Diaminobenzidine (DAB) chromogen was added and monitored microscopically for optimal signal development. Hematoxylin counterstaining (3 minutes) was followed by dehydration (ethanol 75%-100%) and xylene clearing. Whole-slide images were analyzed using Halo software to quantify DAB-positive area percentages from three representative fields per section.

RT-qPCR Assay

Left atrial tissues were homogenized in TRIzol using a high-throughput cryogenic grinder (MB-LD48S, Zhejiang Mibei Instruments Co., Ltd., China). Total RNA was extracted using the RNAeasy Mini Kit (Accurate Biotechnology, Hunan, China), and purity was assessed with a Nano-500 microspectrophotometer (Hangzhou Aosheng Instruments Co., Ltd., China). First-strand cDNA was synthesized using a reverse transcription kit (Accurate Biotechnology), followed by RT-qPCR using SYBR Green Master Mix (Accurate Biotechnology) on a CFX Connect RT-qPCR system (Bio-Rad, USA; 788R06671). Primer sequences are listed in Table 1. Reactions were conducted in 20 μL volumes under the following cycling conditions: 95°F for 30 seconds, then 40 cycles

HIGHLIGHTS

- Vericiguat ameliorates structural remodeling in atrial fibrillation (AF) rats, as shown by attenuated atrial dilation and reduced collagen I deposition.
- Vericiguat demonstrates potent anti-fibrotic and anti-remodeling effects by attenuating atrial dilation and collagen I deposition in a rat model of AF.
- We identify the normalization of dysregulated autophagy as a novel mechanism underlying vericiguat's cardioprotective action.

Table 1. Primer sequences used for quantitative real-time PCR analysis.

Gene	Forward (5'-3')	Reverse (5'-3')
ATG7	AATGATGTGGTGGCTCCAGG	CCTCAGGATGCTGCAAGACA
Collagen I	CACTGCAAGAACAGCGTAGC	AAGTTCCGGTGTGACTCGTG
GAPDH	GGCACAGTCAAGGCTGAGAATG	ATGGTGGTGAAGACGCCAGTA

Gene-specific primers were designed using the NCBI Primer-BLAST tool (https://www.ncbi.nlm.nih.gov/tools/primer-blast/).

of 95°F for 5 seconds, and 60°F for 30 seconds. Each analysis included three independent biological replicates with technical triplicates. Gene expression was normalized to GAPDH and calculated using the $2^{-\Delta\Delta Ct}$ method. Primer design and validation.

The coding sequence of the rat GAPDH, ATG7, collagen I gene was downloaded from the NCBI Nucleotide database. Gene-specific primers were designed using the NCBI Primer-BLAST tool (https://www.ncbi.nlm.nih.gov/tools/primer-blast/). Design parameters were configured as follows: product size range of 70-150 bp, optimal primer length of 20 nucleotides (18-22 range), optimal melting temperature (Tm) of 60°C (58-62°C range), and optimal GC content of 50% (40-60% range). To ensure specificity, the "Primer specificity check" parameter was set to query the Norway rat (taxid:10116) RefSeq mRNA database. From the output, a primer pair spanning an exon-exon junction was selected to preclude genomic DNA amplification and was further evaluated for minimal secondary structure using OligoAnalyzer Tool.

Western Blotting

Total protein was extracted from rat left atrial tissue, and concentrations were quantified using the bicinchoninic acid assay (Beyotime, China). Equal amounts of protein (30 μg/lane) were denatured in 5× sodium dodecyl sulfate (SDS) loading buffer (Solarbio) and separated via 10%-15% gradient SDS-PAGE (80 V for 30 minutes followed by 120 V for 60 minutes). Proteins were then transferred to PVDF membranes (Millipore, USA) at 200 mA for 90 minutes. Membranes were blocked with a protein-free rapid sealing solution (PS108, Epizyme) and incubated overnight at 4°C with primary antibodies against: Collagen I (1:500, AF7001, Affinity), CaMKII (1:4000, 12666-2-AP, Proteintech), Cx43 (1:4000, 26980-1-AP, Proteintech), ATG7 (1:1000, ET1610-53, HuaAn), P62 (1:1000, A7785, ABclonal), LC3B (1:2000, ab192890, Abcam), GAPDH (1:30,000, AC001, ABclonal), and Tubulin (1:3000, 11224-1-AP; Proteintech). After washing with Tris-buffered saline with Tween 20, membranes were incubated with horseradish peroxidase–conjugated goat anti-rabbit IgG (1:10,000, bs-0295G-HRP, Bioss) for 1 hour at room temperature. Signal detection was performed using ECL substrate (Bio-Rad), and images were acquired with a ChemiDoc XR system (Bio-Rad, USA). Band intensities were quantified using Image Lab software (version 6.1). Each analysis included three independent biological replicates

Statistical Analysis

Data analysis was conducted using GraphPad Prism (version 8.01; GraphPad Software, San Diego, CA, USA). Normality of the data was assessed using the Shapiro–Wilk test. Results are presented as mean ± standard deviation (SD). For comparisons between two groups, the Student's *t*-test was used (e.g., for the frequency and duration of AF episodes between the AF and Ver + AF groups), while comparisons among multiple groups were performed using one-way analysis of variance (ANOVA) followed by Tukey's post-hoc test. A *P*-value of less than .05 was considered statistically significant.

RESULTS

Electrocardiogram Analysis

Daily electrocardiographic monitoring was performed on the rats. A total of 16 rats developed paroxysmal AF starting on the seventh day following continuous injection of the ACh-$CaCl_2$ mixture. Atrial fibrillation (AF) induction was characterized by the absence of P waves, the appearance of fibrillatory (f) waves, and irregular RR intervals. Over the subsequent seven days, the frequency and duration of AF episodes following each drug injection were recorded (Table 2). According to the 2024 ESC guidelines on the definition of AF,[1] modeling was successfully established in all 16 rats. These rats were then randomly divided into the AF group and the Ver + AF group, while the control group, which received an equal volume of saline, exhibited no abnormalities in the electrocardiogram (Figure 1C).

Echocardiographic Analysis

After four weeks of continuous vericiguat administration, echocardiographic assessment revealed no significant differences in LVEF or FS between the AF and control groups. However, the LAD was significantly increased in the AF group and was notably reduced following vericiguat treatment (Figure 1A and B; Table 3).

Vericiguat Significantly Attenuated Atrial Fibrillation–Induced Morphological Alterations

Hematoxylin and eosin (HE) staining showed that cardiomyocytes in the control group were well-organized with aligned nuclei, whereas the AF group exhibited disorganized myocardial fibers, necrosis, and inflammatory infiltration. These pathological changes were markedly attenuated by vericiguat (Figure 2A). Masson's trichrome staining revealed significantly elevated collagen deposition and collagen volume fraction (CVF) in the AF group, both of which were significantly reduced by vericiguat treatment (Figure 2B and C).

Table 2. Serum NT-proBNP levels in control, AF, and Ver+AF groups.

	Control	AF	Ver + AF
NT-proBNP (pg/mL)	361 ± 23.75***	790 ± 66.54	560.3 ± 55.12*

*P<.05,**P < .01,***P < .001 vs. atrial fibrillation (AF) group.

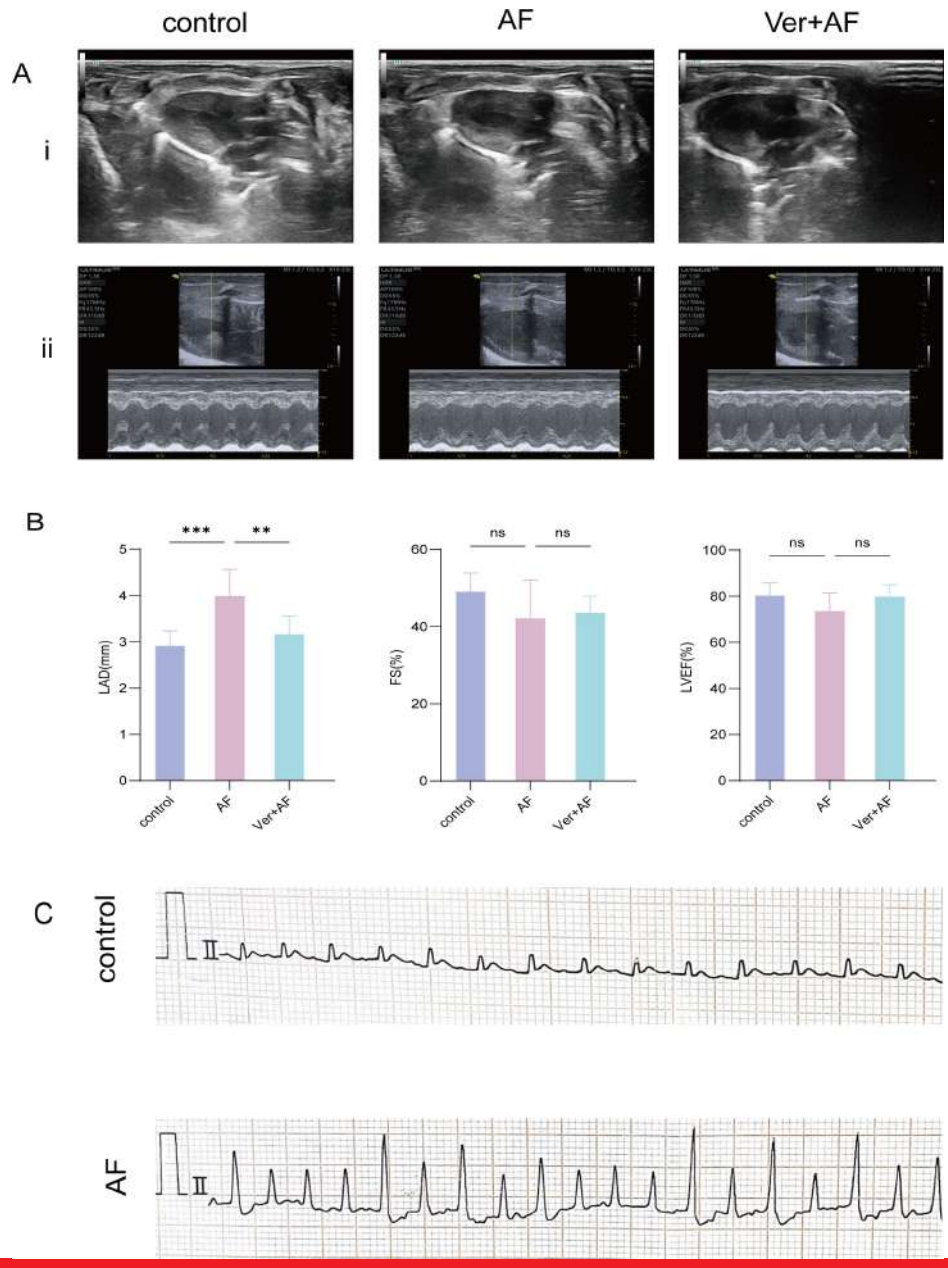

Figure 1. (A) Echocardiographic alterations in experimental groups. i: long axis/B-ultra; ii: short axis/M-ultra. (B) left atrial diameter (LAD mm), left ventricular shortening fraction (FS%), and left ventricular ejection fraction (LVEF%) of rats in each group. Data are presented as mean ± standard deviation. Comparisons among groups were performed using one-way ANOVA. *$P < .01$,*$P < .001$ vs AF group, n = 8 per group. (C) ECG analysis in the atrial fibrillation (AF) group and the control group.**

ELISA Analysis of Serum NT-proBNP in Each Group of Rats

Serum NT-proBNP levels were significantly elevated in the AF group and were substantially reduced following vericiguat treatment (Figure 2D; Table 4).

Vericiguat Attenuated the Upregulation of Collagen I and CaMKII, as well as the Downregulation of Cx43, in the AF Model

Western blot, immunohistochemistry (IHC), and RT-qPCR analyses demonstrated that the AF group exhibited upregulation of Collagen I and CaMKII, along with downregulation

Table 3. Echocardiographic parameters in control, AF, and Ver+AF groups

	Control	AF	Ver + AF
Left atrial diameter (mm)	2.886 ± 0.345***	4.389 ± 0.917	3.475 ± 0.377*
FS(%)	48.64 ± 4.399	42.4 ± 9.505	43.97 ± 4.215
EF(%)	79.02 ± 3.742	74.33 ± 7.681	78.12 ± 3.854

*P<0.05,**P < 0.01,***P < 0.001 vs atrial fibrillation (AF) group.
AF, atrial fibrillation; EF, ejection fraction (%); FS, fractional shortening (%); LAD, left atrial diameter (mm).

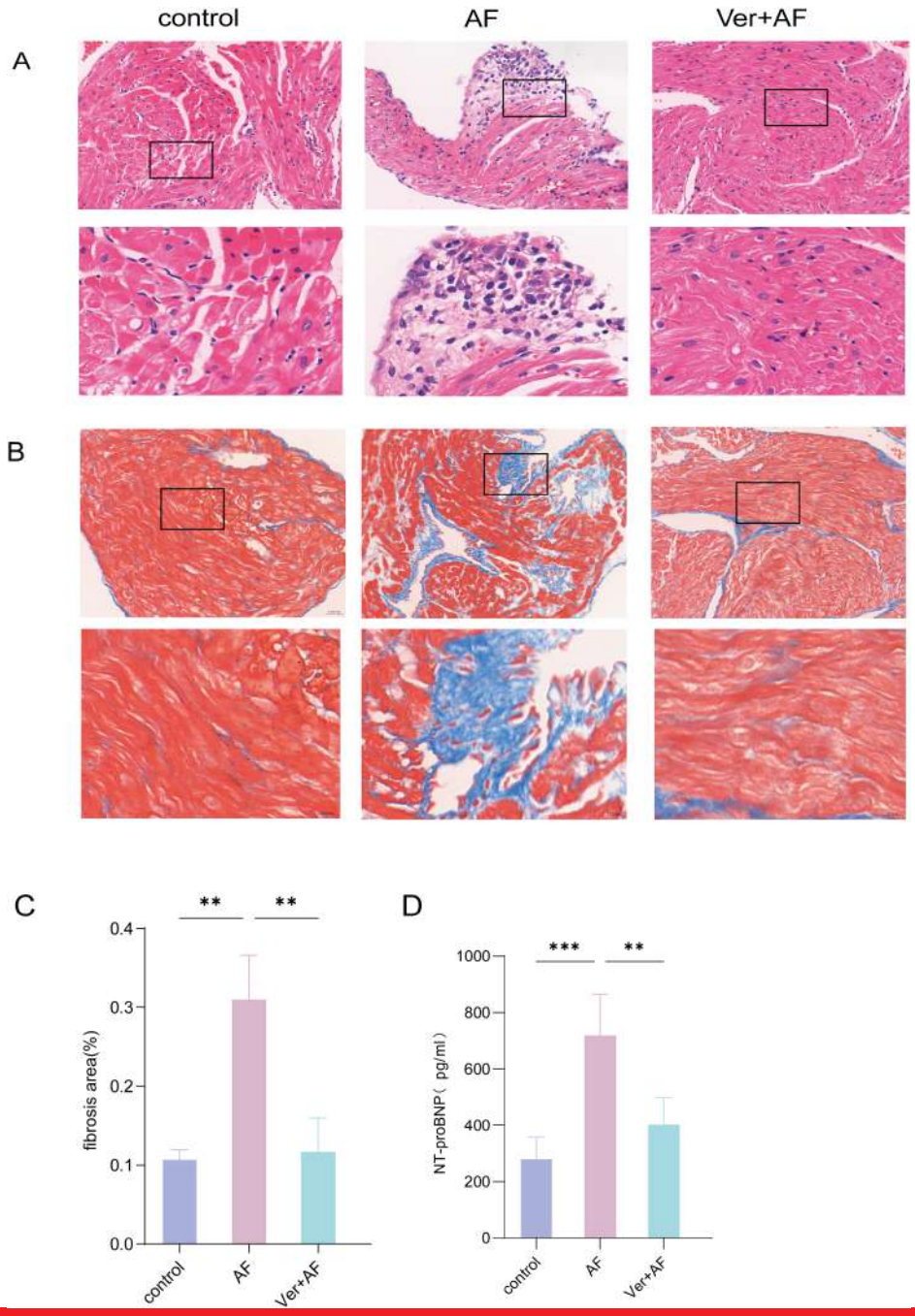

Figure 2. Histological and serological changes in rat myocardial tissues: (A) Representative images of HE-stained left atrial tissues from each group. (B) Masson-stained left atrial tissues across experimental groups. (C) Collagen volume fraction (CVF%) in the left atrium (magnification: 40× and 100×). (D) Serum NT-proBNP levels in different groups. Data are presented as mean ± standard deviation. Comparisons among groups were performed using one-way ANOVA. *$P<.05$, **$P<.01$, ***$P<.001$ vs atrial fibrillation (AF) group. n = 3 per group for panels A-C, n = 5 for panel D.

of Cx43. Vericiguat effectively reversed these changes ($P < .05$ vs. AF group; Figure 3A-G), indicating its role in modulating both electrical and structural remodeling in AF.

Vericiguat Suppressed the Upregulation of ATG7 and LC3II/I, as well as the Downregulation of P62

Consistent with this, expression of autophagy-related proteins was altered in the AF group, with significant upregulation of ATG7 and LC3II/I and downregulation of P62. Vericiguat treatment reversed these trends (Figure 4A-G), suggesting that its therapeutic mechanism may involve suppression of pathological autophagy activation in AF.

DISCUSSION

Key findings of this study are as follows: (1) AF rats exhibited significantly increased collagen I expression and left

Table 4. Comparison of atrial fibrillation frequency and duration between AF and Ver+AF groups.

	Average Frequency (Time)/Seven Days	Average Duration (s)/ Seven Days
AF	7.339 ± 0.481	348.6 ± 5.721
Ver + AF	7.268 ± 0.524	350.4 ± 8.029
P value	.783 (ns)	.614 (ns)

Data are expressed as mean ± standard deviation. Comparisons between two groups were performed using Student's *t*-test; ns indicates no statistically significant difference (*P*> .05).
AF, atrial fibrillation.

atrial diameter, both of which were attenuated by vericiguat treatment. (2) Elevated CaMKII expression and decreased connexin 43 (Cx43) levels in AF rats were reversed with vericiguat administration. (3) Dysregulation of autophagy-related proteins—upregulation of LC3II/I and ATG7, and downregulation of P62—was normalized by vericiguat, implicating autophagy modulation as a potential mechanism of action.

Calcium/calmodulin-dependent protein kinase II (CaMKII) plays a central role in atrial electrical remodeling by phosphorylating ryanodine receptor 2 (RyR2), thereby enhancing sarcoplasmic reticulum calcium release and promoting intracellular calcium overload. This leads to shortened APD and aberrant electrical activity that facilitates AF initiation and perpetuation.[22,23] Connexin 43 (Cx43), the principal gap junction protein in atrial myocytes, ensures coordinated impulse propagation.[24] Its downregulation or disorganization disrupts electrical conduction, creating a substrate for microreentry and arrhythmia maintenance.[25] Notably, excessive autophagy has been shown to suppress Cx43 expression, linking proteostatic imbalance to arrhythmogenesis.[26] Atrial fibrosis, characterized by extracellular matrix expansion and disorganized collagen I deposition,[27,28] impairs conduction homogeneity and promotes delayed depolarization, increasing vulnerability to reentrant arrhythmias. This fibrotic remodeling not only initiates AF but also sustains its recurrence by establishing a persistent arrhythmogenic substrate.

Autophagy is a regulated catabolic process that facilitates the degradation and recycling of intracellular components via lysosomal pathways. It is activated by stressors such as oxidative stress, hypoxia, and nutrient deprivation. Upon activation, the ULK1 complex initiates autophagosome formation, and ATG7 promotes the lipidation of LC3-I to

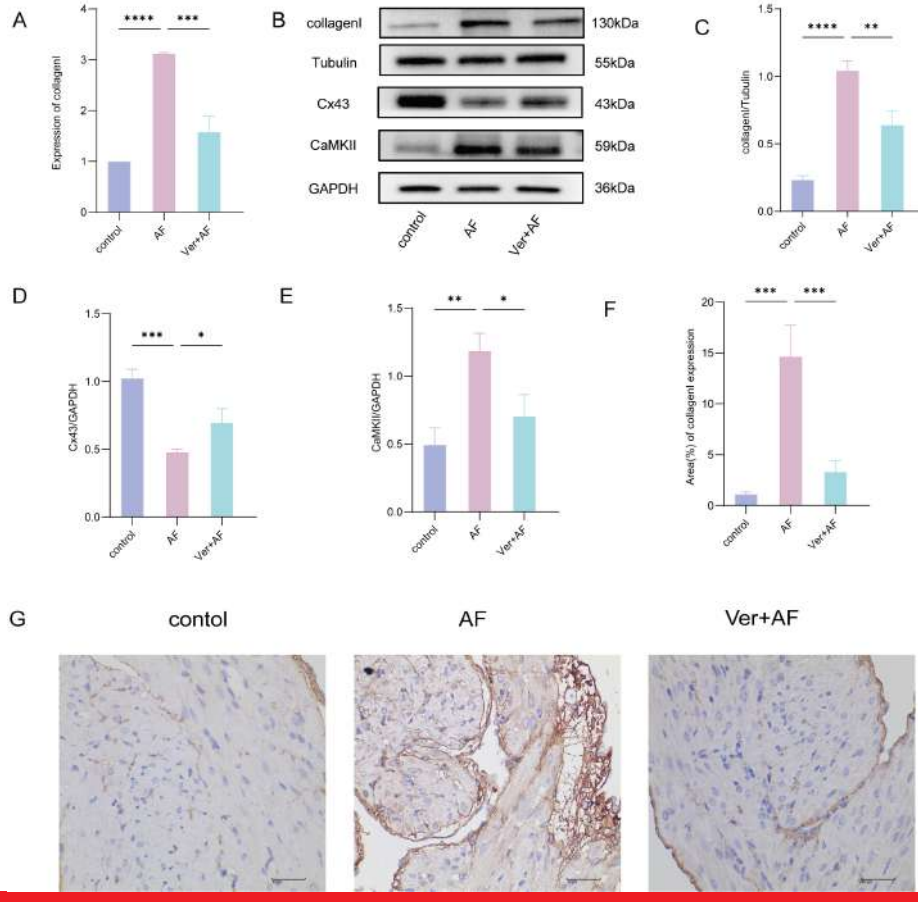

Figure 3. (A) RT-qPCR analysis of Collagen I mRNA expression levels across experimental groups. (B-E) Western blot quantification of Collagen I, Cx43, and CaMKII protein levels. (F, G) Representative immunohistochemical (IHC) images showing Collagen I deposition (magnification: 40×; n = 3 per group). Data are presented as mean ± standard deviation. Comparisons among groups were performed using one-way ANOVA. *P<.05, **P < 0.05, **P < .01, ***P < .001, ****P < .0001 vs. atrial fibrillation (AF) group.

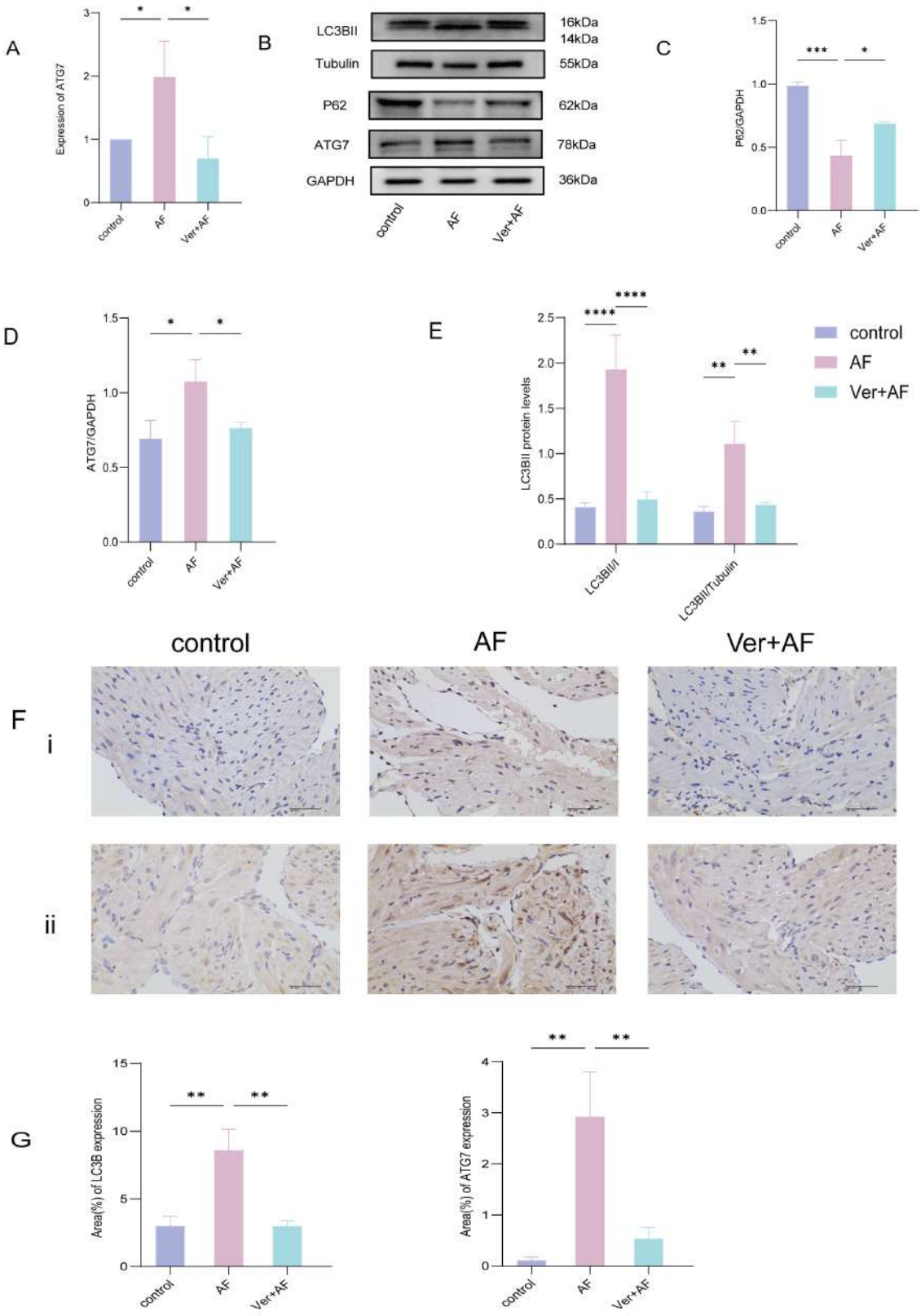

Figure 4. (A) RT-qPCR analysis of ATG7 mRNA expression levels across experimental groups. (B–E) Western blot quantification of ATG7, P62, and LC3II/I protein expression levels. (F,G) Representative immunohistochemical (IHC) images showing tissue-specific expression of (i) ATG7 and (ii) LC3II/I (magnification: 40×; n = 3 per group). Data are presented as mean ± standard deviation. Comparisons among groups were performed using one-way ANOVA. *P<.05, **P < 0.01, ***P < .001 vs. atrial fibrillation (AF) group.

form LC3-II. LC3-II then incorporates into autophagosomal membranes, aiding in the sequestration of cytoplasmic substrates. Concurrently, p62/SQSTM1 binds to ubiquitinated cargo and anchors it to autophagosomes. Mature autophagosomes fuse with lysosomes for the degradation and recycling of metabolic byproducts.[29,30] Excessive autophagy promotes atrial fibrosis through mechanisms like increased extracellular matrix deposition and collagen I overproduction, which facilitate AF persistence and recurrence.[10,31-33]

To characterize fibrotic remodeling, we comprehensively assessed atrial collagen I deposition across experimental groups using multiple modalities. The AF group exhibited significantly elevated collagen I expression and increased CVF relative to controls, corroborating previous reports linking fibrosis to AF progression.[16,34,35] Echocardiographic analysis further revealed marked left atrial enlargement in AF rats, while LVEF and FS remained unaltered. In parallel, serum NT-proBNP levels—a biomarker of myocardial stress—were significantly elevated in the AF cohort. Notably, vericiguat treatment attenuated these pathological changes, consistent with its documented benefits in mitigating ventricular remodeling in HF models.[36] Given the contributions of CaMKII upregulation and connexin 43 (Cx43) downregulation to atrial electrical remodeling, we quantified their expression profiles. Atrial fibrillation (AF) was associated with pronounced increases in CaMKII expression and concomitant reductions in Cx43 levels, indicative of impaired calcium handling and disrupted gap junctional communication. Vericiguat administration reversed these molecular derangements, suggesting its capacity to restore electrophysiological stability by simultaneously modulating calcium signaling and intercellular connectivity.

Furthermore, we observed distinct alterations in autophagy-related markers in the AF group: a significantly elevated LC3II/I ratio, increased mRNA and protein expression of *ATG7*, and reduced levels of p62. These changes suggest a shift in autophagic activity, indicating that paroxysmal AF may lead to changes in autophagic activity in atrial cardiomyocytes, in line with previous findings.[9,37,38] These observations suggest that restoring autophagic balance might help reduce AF susceptibility. Our study demonstrated that vericiguat reversed the alterations in the above proteins.

In summary, our study provides evidence that vericiguat may alleviate paroxysmal AF, potentially through modulation of atrial autophagy.

Limitations

However, our study has several limitations. The relatively small sample size, particularly in histological and molecular analyses, may limit the generalizability of our findings. Additionally, we focused solely on the effects of vericiguat in a paroxysmal AF model, and future studies should evaluate its mechanisms in other AF subtypes, such as persistent AF.

AI Disclosure: The authors declare that no generative AI tools (such as large language models, chatbots, or image creators) were used in any stage of the preparation or writing of this manuscript.

Ethics Committee Approval: Animal Ethics Statement: Twenty-four male Sprague Dawley rats (8 weeks old, 250–300 g) were obtained from the Animal Experiment Center of North Sichuan Medical College and approved by the Ethics Committee of North Sichuan Medical College (License No.: SYXK[Sichuan]2023-0076, Nanchong, China). All procedures adhered to the Guidelines for the Care and Use of Laboratory Animals and were approved by the Animal Ethics Committee of North Sichuan Medical College (Approval No. [2024]005). Efforts were made to minimize animal suffering.

Peer-review: Externally peer-reviewed.

Acknowledgments: We want to express our gratitude to the Science and Technology Innovation Center of North Sichuan Medical College, as well as the Institute of Hepatobiliary and Pancreatic Diseases and the Affiliated Hospital of North Sichuan Medical College.

Author Contributions: Concept – Y.Y., Y.W.; Design – Y.W., X.Z.; Supervision – Y.W.; Resources – Y.W.; Materials – X.Z., L.S.; Data Collection and/or Processing – X.Z., L.S, W.L.; Analysis and/or Interpretation – X.Z., Z.S., Q.W.; Literature Search – Y.C., Y.Y., H.L.; Writing – X.Z., L.S.; Critical Review – Y.W.

Declaration of Interests: The authors have no conflicts of interest to declare.

Funding: The authors declare that this study received no financial support.

REFERENCES

1. Van Gelder IC, Rienstra M, Bunting KV, et al. 2024 ESC Guidelines for the management of atrial fibrillation developed in collaboration with the European Association for Cardio-Thoracic Surgery (EACTS). *Eur Heart J*. 2024;45(36):3314-3414. [CrossRef]
2. Erol Ç. Focus on arrhythmias. *Anatol J Cardiol*. 2025;29(5):209. [CrossRef]
3. Yang H, Xiang J, Shen J, Tang B, Zhang L. Global research trends of cryoablation for atrial fibrillation from 2002 to 2022: A bibliometric analysis. *Anatol J Cardiol*. 2023;27(12):688-696. [CrossRef]
4. Brundel BJJM, Ai X, Hills MT, Kuipers MF, Lip GYH, de Groot NMS. Atrial fibrillation. *Nat Rev Dis Primers*. 2022;8(1):21. [CrossRef]
5. Odutayo A, Wong CX, Hsiao AJ, Hopewell S, Altman DG, Emdin CA. Atrial fibrillation and risks of cardiovascular disease, renal disease, and death: systematic review and meta-analysis. *BMJ*. 2016;354:i4482. [CrossRef]
6. Sagris M, Vardas EP, Theofilis P, Antonopoulos AS, Oikonomou E, Tousoulis D. Atrial fibrillation: pathogenesis, predisposing factors, and genetics. *Int J Mol Sci*. 2021;23(1):6. [CrossRef]
7. Pirruccello JP, Di Achille P, Choi SH, et al. Deep learning of left atrial structure and function provides link to atrial fibrillation risk. *Nat Commun*. 2024;15(1):4304. [CrossRef]
8. Yamaguchi T. Atrial structural remodeling and atrial fibrillation substrate: A histopathological perspective. *J Cardiol*. 2024;85(2):47-55. [CrossRef]
9. Yuan Y, Zhao J, Gong Y, et al. Autophagy exacerbates electrical remodeling in atrial fibrillation by ubiquitin-dependent degradation of L-type calcium channel. *Cell Death Dis*. 2018;9(9):873. [CrossRef]
10. Frangogiannis NG. Cardiac fibrosis. *Cardiovasc Res*. 2021;117(6):1450-1488. [CrossRef]
11. Armstrong PW, Pieske B, Anstrom KJ, et al. Vericiguat in patients with heart failure and reduced ejection fraction. *N Engl J Med*. 2020;382(20):1883-1893. [CrossRef]
12. Ponikowski P, Alemayehu W, Oto A, et al. Vericiguat in patients with atrial fibrillation and heart failure with reduced ejection

fraction: insights from the Victoria trial. *Eur J Heart Fail*. 2021;23(8):1300-1312. [CrossRef]
13. Coats AJS, Tolppanen H. Drug treatment of heart failure with reduced ejection fraction: defining the role of vericiguat. *Drugs*. 2021;81(14):1599-1604. [CrossRef]
14. Hulot J-S, Trochu J-N, Donal E, et al. Vericiguat for the treatment of heart failure: mechanism of action and pharmacological properties compared with other emerging therapeutic options. *Expert Opin Pharmacother*. 2021;22(14):1847-1855. [CrossRef]
15. Kassis-George H, Verlinden NJ, Fu S, Kanwar M. Vericiguat in heart failure with a reduced ejection fraction: patient selection and special considerations. *Ther Clin Risk Manag*. 2022;18:315-322. [CrossRef]
16. Lou Q, Li L, Liu G, et al. Vericiguat reduces electrical and structural remodeling in a rabbit model of atrial fibrillation. *J Cardiovasc Pharmacol Ther*. 2023;28:10742484231185252. [CrossRef]
17. Wei F, Ren W, Zhang X, Wu P, Fan J. miR-425-5p is negatively associated with atrial fibrosis and promotes atrial remodeling by targeting CREB1 in atrial fibrillation. *J Cardiol*. 2022;79(2):202-210. [CrossRef]
18. Feng R, Wan J, He Y, Gong H, Xu Z, Feng J. Angiotensin-receptor blocker losartan alleviates atrial fibrillation in rats by downregulating frizzled 8 and inhibiting the activation of WNT-5A pathway. *Clin Exp Pharmacol Physiol*. 2023;50(1):19-27. [CrossRef]
19. Zeng X, Zhang H, Xu T, et al. Vericiguat attenuates doxorubicin-induced cardiotoxicity through the PRKG1/PINK1/STING axis. *Transl Res*. 2024;273:90-103. [CrossRef]
20. Chen W, Wu Y, Li W, et al. Vericiguat improves cardiac remodelling and function in rats with doxorubicin-induced cardiomyopathy. *ESC Heart Fail*. 2025;12(3):1807-1817. [CrossRef]
21. Li C, Zheng C, Pu Y, et al. Vericiguat enhances the therapeutic efficacy of mesenchymal stem cells-derived exosomes in acute myocardial infarction through microRNA-1180-3p/ETS1 pathway. *Cell Signal*. 2025;125:111512. [CrossRef]
22. Nattel S, Heijman J, Zhou L, Dobrev D. Molecular basis of atrial fibrillation pathophysiology and therapy: A translational perspective. *Circ Res*. 2020;127(1):51-72. [CrossRef]
23. Heijman J, Muna AP, Veleva T, et al. Atrial myocyte NLRP3/CaMKII nexus forms a substrate for postoperative atrial fibrillation. *Circ Res*. 2020;127(8):1036-1055. [CrossRef]
24. Yoder MW, Wright NT, Borzok MA. Calpain regulation and dysregulation-its effects on the intercalated disk. *Int J Mol Sci*. 2023;24(14):11726. [CrossRef]
25. Nagibin V, Egan Benova T, Viczenczova C, et al. Ageing related down-regulation of myocardial connexin-43 and up-regulation of MMP-2 may predict propensity to atrial fibrillation in experimental animals. *Physiol Res*. 2016;65(suppl 1):S91-S100. [CrossRef]
26. Chen Y, Qiao X, Zhang L, Li X, Liu Q. Apelin-13 regulates angiotensin II-induced Cx43 downregulation and autophagy via the AMPK/mTOR signaling pathway in HL-1 cells. *Physiol Res*. 2020;69(5):813-822. [CrossRef]
27. Odeh A, Dungan GD, Darki A, et al. Collagen remodeling and fatty acid regulation biomarkers in understanding the molecular pathogenesis of atrial fibrillation. *Clin Appl Thromb Hemost*. 2022;28:10760296221145181. [CrossRef]
28. Takahashi Y, Yamaguchi T, Otsubo T, et al. Histological validation of atrial structural remodelling in patients with atrial fibrillation. *Eur Heart J*. 2023;44(35):3339-3353. [CrossRef]
29. Li W, He P, Huang Y, et al. Selective autophagy of intracellular organelles: recent research advances. *Theranostics*. 2021;11(1):222-256. [CrossRef]
30. Tanida I. Autophagosome formation and molecular mechanism of autophagy. *Antioxid Redox Signal*. 2011;14(11):2201-2214. [CrossRef]
31. Xu X, Jiang R, Chen M, et al. Puerarin decreases collagen secretion in AngII-induced atrial fibroblasts through inhibiting autophagy via the JNK-Akt-mTOR signaling pathway. *J Cardiovasc Pharmacol*. 2019;73(6):373-382. [CrossRef]
32. Wang H, Yang X, Yang Q, Gong L, Xu H, Wu Z. PARP-1 inhibition attenuates cardiac fibrosis induced by myocardial infarction through regulating autophagy. *Biochem Biophys Res Commun*. 2018;503(3):1625-1632. [CrossRef]
33. Ghavami S, Cunnington RH, Gupta S, et al. Autophagy is a regulator of TGF-β1-induced fibrogenesis in primary human atrial myofibroblasts. *Cell Death Dis*. 2015;6(3):e1696. [CrossRef]
34. Li L-Y-F, Lou Q, Liu G-Z, et al. Sacubitril/valsartan attenuates atrial electrical and structural remodelling in a rabbit model of atrial fibrillation. *Eur J Pharmacol*. 2020;881:173120. [CrossRef]
35. Sun X, Sheng Y, Xu P, Peng Q, Ruan Z. Vericiguat reduces atrial fibrillation recurrence by alleviating myocardial fibrosis via the TGF-β1/Smad2/3 pathway. *PLOS One*. 2025;20(7):e0328272. [CrossRef]
36. Armstrong PW, Zheng Y, Troughton RW, et al. Sequential evaluation of NT-proBNP in heart failure: insights into clinical outcomes and efficacy of vericiguat. *JACC Heart Fail*. 2022;10(9):677-688. [CrossRef]
37. Wiersma M, Meijering RAM, Qi X-Y, et al. Endoplasmic reticulum stress is associated with autophagy and cardiomyocyte remodeling in experimental and human atrial fibrillation. *J Am Heart Assoc*. 2017;6(10):e006458. [CrossRef]
38. Fedai H, Altiparmak IH, Tascanov MB, et al. The relationship between oxidative stress and autophagy and apoptosis in patients with paroxysmal atrial fibrillation. *Scand J Clin Lab Investig*. 2022;82(5):391-397. [CrossRef]